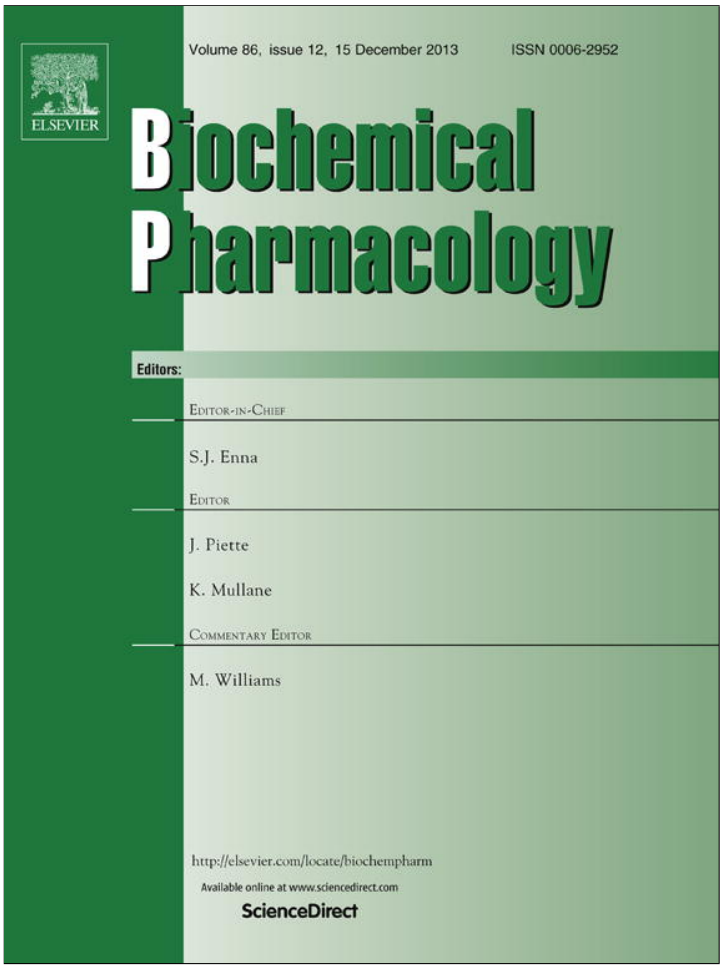

Biochemical Pharmacology 86 (2013) 1699–1707

Contents lists available at ScienceDirect

Biochemical Pharmacology

journal homepage: www.elsevier.com/locate/biochempharm

Pharmacokinetics and *in vivo* antistaphylococcal efficacy of TXY541, a 1-methylpiperidine-4-carboxamide prodrug of PC190723

Malvika Kaul [a], Lilly Mark [b,c], Yongzheng Zhang [b], Ajit K. Parhi [b], Edmond J. LaVoie [c], Daniel S. Pilch [a,*]

[a] Department of Pharmacology, Rutgers Robert Wood Johnson Medical School, Piscataway, NJ 08854-5635, United States
[b] Taxis Pharmaceuticals, Inc., North Brunswick, NJ 08902, United States
[c] Department of Medicinal Chemistry, Ernest Mario School of Pharmacy, Rutgers-The State University of New Jersey, Piscataway, NJ 08855, United States

ARTICLE INFO

Article history:
Received 4 September 2013
Accepted 14 October 2013
Available online 20 October 2013

Keywords:
FtsZ
MRSA
Systemic infection
Antibiotics
Drug solubility

ABSTRACT

The benzamide derivative PC190723 was among the first of a promising new class of FtsZ-directed antibacterial agents to be identified that exhibit potent antistaphylococcal activity. However, the compound is associated with poor drug-like properties. As part of an ongoing effort to develop FtsZ-targeting antibacterial agents with increased potential for clinical utility, we describe herein the pharmacodynamics, pharmacokinetics, *in vivo* antistaphylococcal efficacy, and mammalian cytotoxicity of TXY541, a novel 1-methylpiperidine-4-carboxamide prodrug of PC190723. TXY541 was found to be 143-times more soluble than PC190723 in an aqueous acidic vehicle (10 mM citrate, pH 2.6) suitable for both oral and intravenous *in vivo* administration. In staphylococcal growth media, TXY541 converts to PC190723 with a half-life of approximately 8 h. In 100% mouse serum, the TXY541-to-PC190723 conversion was much more rapid (with a half-life of approximately 3 min), suggesting that the conversion of the prodrug in serum is predominantly enzyme-catalyzed. Pharmacokinetic analysis of both orally and intravenously administered TXY541 in mice yielded a half-life for the PC190723 conversion product of 0.56 h and an oral bioavailability of 29.6%. Whether administered orally or intravenously, TXY541 was found to be efficacious *in vivo* in mouse models of systemic infection with both methicillin-sensitive and methicillin-resistant *S. aureus*. Toxicological assessment of TXY541 against mammalian cells revealed minimal detectable cytotoxicity. The results presented here highlight TXY541 as a potential therapeutic agent that warrants further pre-clinical development.

1. Introduction

The spread of infections caused by multidrug-resistant (MDR) bacterial pathogens, such as methicillin-resistant *Staphylococcus aureus* (MRSA), vancomycin-resistant enterococci (VRE), and extended spectrum β-lactamase (ESBL)-producing enterobacteriaceae, has created a need for new antibiotics with novel mechanisms of action [1–4]. FtsZ is a central protein that plays a key role in bacterial cell division (cytokinesis) [5]. Upon binding GTP, it self-polymerizes to form a ring-like structure (the Z-ring) at the bacterial midcell [6–8]. This structure is tethered to the bacterial membrane, and acts as a scaffold for the recruitment of other cytokinetic proteins [9–11]. Mutational studies have indicated that a functional FtsZ gene is essential for bacterial viability [12,13]. The essential role that FtsZ plays in bacterial cell division has made it an attractive new target for antibiotic development that is not exploited by any current clinical agent [14–28].

Among the first FtsZ-targeting antibacterial agents to be identified was the benzamide derivative PC190723 (see structure in Fig. 1) [17]. It exhibits potent activity against staphylococci and bacilli *in vitro*, but has poor activity against enterococci, streptococci, and Gram-negative species [14,16,17,27,29]. This spectrum of activity appears to be correlated with the FtsZ-targeting specificity of the compound [29,30]. Despite its initial promise, the pre-clinical development of PC190723 and related benzamide compounds has been hampered by poor formulation properties. As part of an ongoing effort to develop more druggable benzamide analogs, we report here the synthesis and characterization of a *N*-(3-((6-chlorothiazolo[5,4-*b*]pyridin-2-yl)methoxy)-2,6-difluorobenzoyl)-1-methylpiperidine-4-carboxamide derivative (TXY541 - see structure in Fig. 1) that acts as a prodrug of PC190723 in serum. It is associated with enhanced drug-like properties and antistaphylococcal efficacy *in vivo* with both intravenous and oral administration.

* Corresponding author.
E-mail addresses: pilchds@rwjms.rutgers.edu, daniel.pilch@rutgers.edu (D.S. Pilch).

0006-2952/$ – see front matter © 2013 Elsevier Inc. All rights reserved.
http://dx.doi.org/10.1016/j.bcp.2013.10.010

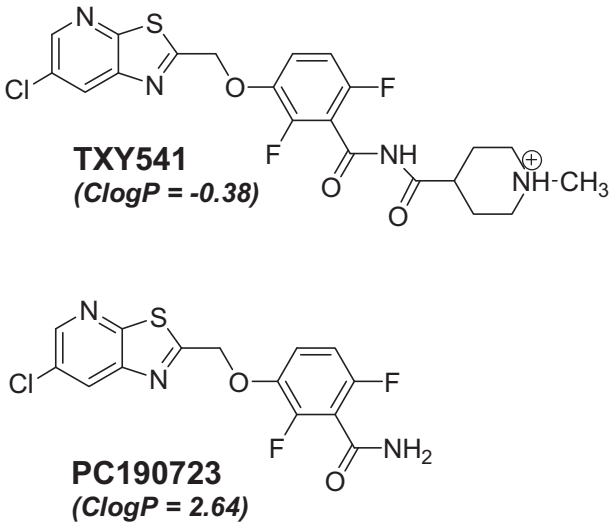

Fig. 1. Structures of TXY541 and PC190723. TXY541 is depicted with the methylpiperidine functionality in its protonated (cationic) form. The indicated *C* log *P* values were calculated using the weighted method (VG = KLOP = PHYS = 1) in the Marvin 5.12 Software Suite (ChemAxon, Ltd.), with Cl^- and Na^+/K^+ concentrations being set at 0.1 mol/dm^3.

2. Materials and methods

2.1. Bacterial strains and comparator antibiotics

S. aureus 8325-4 was a gift from Dr. Glenn W. Kaatz (John D. Dingell VA Medical Center, Detroit, MI) [31]. All other *S. aureus* strains were obtained from the American Type Culture Collection (ATCC, Manassas, VA). Vancomycin HCl, oxacillin (sodium salt), and erythromycin were obtained from Sigma–Aldrich Co. (St. Louis, MO).

2.2. General chemistry methods and synthesis of PC190723 and TXY541

All reactions were done under nitrogen atmosphere. Reaction monitoring and follow-up were done using aluminum backed Silica G TLC plates with UV254 (Sorbent Technologies, Norcross, GA), and visualizing with ultraviolet light. Flash column chromatography was done on a CombiFlash Rf (Teledyne ISCO, Lincoln, NE). The ^{1}H (300 MHz) and ^{13}C (75 MHz) NMR spectra were acquired on a Varian Unity Inova (300 MHz) multinuclear NMR spectrometer. Data are expressed in parts per million relative to the residual nondeuterated solvent signals, and spin multiplicities are given as s (singlet) or m (multiplet). Melting points were determined using a Mel-Temp II apparatus (Laboratory Devices, Inc., Holliston, MA) and are uncorrected. Unless otherwise indicated, all solvents and chemicals were obtained from Sigma–Aldrich, Co.

PC190723 was synthesized as previously described [32]. 0.5 g of *N*-methylisonipecotic acid hydrochloride (Combi-Blocks, Inc., San Diego, CA) was dissolved in 1.5 mL of dry $SOCl_2$. The mixture was then heated at 80 °C for 2 h under argon. Cooling and evaporation to dryness afforded *N*-methylisonipecotyl chloride as a yellow solid, which was used without further purification. To a mixture of PC190723 (400 mg, 1.12 mmol) and *N*-methylisonipecotyl chloride (HCl salt) (400 mg, 2.02 mmol) in 20.0 mL of dry tetrahydrofuran (THF) was added NaH (200 mg, 5.0 mmol, 60% dispersion in mineral oil) at room temperature. The resulting reaction mixture was stirred at room temperature overnight. After completion of the reaction, it was quenched by the addition of a few drops of 1 N NaOH, and diluted with ethyl acetate. The organic phase was separated, washed successively with saturated $NaHCO_3$ brine, and dried (with anhydrous Na_2SO_4). The solvent was removed under reduced pressure. The resulting residue was purified using an ISCO chromatograph [with 10% MeOH in dichloromethane (DCM) + 1% NH_4OH as the eluent] to afford *N*-(3-((6-chlorothiazolo[5,4-*b*]pyridin-2-yl)methoxy)-2,6-difluorobenzoyl)-1-methylpiperidine-4-carboxamide (TXY541) as a yellow solid (300 mg, 56% Yield): mp 204–207 °C; ^{1}H NMR (300 MHz, $CDCl_3$) δ: 8.58 (s, 1H), 8.28 (s, 1H), 7.23–7.15 (m, 1H), 6.95–6.88 (m, 1H), 5.48 (s, 2H), 2.94–2.85 (m, 3H), 2.30 (s, 3H), 2.10–1.76 (m, 6H). ^{13}C NMR (75 MHz, DMSO-d_6) δ: 175.6, 172.5, 171.4, 161.1, 156.3, 151.4, 146.9, 146.6, 142.5, 130.7, 130.0, 118.3, 112.1, 111.8, 69.9, 55.1, 42.7, 28.4. The high resolution mass spectrometry (HRMS) for $C_{21}H_{19}ClF_2N_4O_3S$ $(M+H)^+$ was calculated to be 481.0907, while being found to be 481.0911. The molecular weights of TXY541 and PC190723 are 479.93 and 354.76, respectively.

2.3. Compound solubility studies

The maximum solubility of TXY541 in 10 mM citrate (pH 2.6) or phosphate-buffered saline (PBS) (pH 7.4) was determined at 25 °C. In this assay, the compound was combined with vehicle at a w/v ratio above its solubility limit, and the amount of dissolved compound quantified. Each solubility assessment was conducted in duplicate. All samples were vortexed for 3 min to afford maximal compound dissolution and then centrifuged at 16,000 × *g* for 1 min to pellet out any unsolubilized compound. The concentration of compound in each of the resulting supernatants was then quantified using reverse-phase high-performance liquid chromatography (HPLC) as described below, and generating standard curves of peak area *versus* compound concentration (in the appropriate vehicle). Citrate was obtained from Sigma–Aldrich, Co., and PBS was obtained from Lonza (Walkersville, MD).

2.4. Compound stability studies

Experimental solutions of TXY541 or PC190723 at concentrations of 20 μM were prepared from 4 mg/mL DMSO stock solutions in either cation-adjusted Mueller-Hinton (CAMH) broth (pH 7.4), 100% filtered mouse serum (pH 7.4), or 10 mM citrate (pH 2.6). The relative amount of TXY541 and PC190723 in each experimental solution was then assessed as a function of time at 37 °C using reverse-phase HPLC as described below. CAMH broth was obtained from Becton, Dickinson and Co. (Franklin Lakes, NJ), and filtered mouse serum was obtained from Lampire Biological Laboratories, Inc. (Ottsville, PA).

2.5. Reverse-phase HPLC

For all HPLC measurements, a reverse-phase SPHER-100 C18 column (Princeton Chromatography, Inc.) was used on a Shimadzu LC-20AT liquid chromatograph equipped with a Shimadzu SPD-20AV UV/VIS detector (set at 296 nm). The column size was 150 mm × 4.6 mm, with the particle and pore sizes being 5 μm and 100 Å, respectively. A 20 μL sample of each experimental solution was injected and a flow rate of 1 mL/min was applied, along with a gradient of 10–90% acetonitrile [containing 0.1% (v/v) trifluoroacetic acid (TFA)] and water in the mobile phase. The total run time was 20 min, with the sampling frequency and response time being 2 Hz and 1 s, respectively. Peak areas were determined using the Shimadzu EZStart 7.4 SP3 software package.

2.6. Minimum inhibitory concentration (MIC) assays

MIC assays were conducted in accordance with Clinical and Laboratory Standards Institute (CLSI) guidelines for broth microdilution [33]. Briefly, log-phase *S. aureus* bacteria were added to

96-well microtiter plates (at 5×10^5 CFU/mL) containing two-fold serial dilutions of compound or comparator drug (vancomycin, oxacillin, or erythromycin) in CAMH broth. Compound and drug concentrations (each concentration being present in duplicate) ranged from 8 to 0.008 μg/mL in all assays except for the MRSA assays with oxacillin and erythromycin, in which the drug concentrations ranged from 64 to 0.063 μg/mL. The final volume in each well was 0.1 mL, and the microtiter plates were incubated aerobically for 24 h at 37 °C. Bacterial growth was then monitored by measuring OD_{600} using a VersaMax plate reader (Molecular Devices, Inc., Sunnyvale, CA), with the MIC being defined as the lowest compound concentration at which growth was ≥90% inhibited compared to antibiotic-free control. The following *S. aureus* strains were included in these assays: 8325-4 (MSSA), ATCC 19636 (MSSA), ATCC 33591 (MRSA), and ATCC 43300 (MRSA). As recommended by CLSI [33], the CAMH broth was supplemented with 2% NaCl in all the MRSA experiments. When present, filtered mouse serum was used at 50% (v/v).

2.7. Minimum bactericidal concentration (MBC) assays

MBC assays were conducted in accordance with CLSI guidelines [33]. Broth microdilution assays were conducted as described in the preceding section. After the 24 h incubation period, aliquots from the microtiter wells were plated on to tryptic soy agar (TSA; Becton, Dickinson and Co.). The colonies that grew after 24 h of incubation were counted using an Acolyte colony counter (Synbiosis, Inc., Frederick, MD), with MBC being defined as the lowest compound concentration resulting in a ≥3-log reduction in the number of colony forming units (CFUs) [33].

2.8. Assay for the frequency of resistance (FOR)

The frequency of resistance to TXY541 was assayed using a large inoculum approach. In this approach, TSA plates containing TXY541 at concentrations ranging from 4- to 8-times MIC were prepared. A large inoculum of $\sim 7 \times 10^9$ CFU/mL *S. aureus* 8325-4 was spread onto each plate. The colony count of the inoculum was verified by plating serial dilutions of the culture onto non-selective TSA plates. All plates were incubated at 37 °C overnight and examined after 24 h. Mutational frequency was calculated from the ratio of the number of colonies observed on the selective plates to the total number of plated bacteria [34].

2.9. Pharmacokinetic studies

Pharmacokinetic experiments were conducted by SAI Life Sciences Ltd. (Pune, India) in accordance with guidelines established by the Indian Committee for the Purpose of Control and Supervision of Experiments on Animals (CPCSEA). Approval by the Institutional Animal Ethics Committee (IAEC) was obtained prior to initiation of the studies. Healthy male BALB/c mice (8–12 weeks old and weighing between 25 g and 35 g) were obtained from ACTREC (Mumbai, India). Twelve mice were divided into two groups of six mice each, with three mice being housed per cage. Food and water were provided to the mice *ad libitum*. The first group of mice received a single intravenous (i.v.) dose of 24 mg/kg TXY541 by tail vein injection. The second group received single oral (p.o.) dose of 32 mg/kg TXY541 by gavage. In both cases, the compound was formulated in 10 mM citrate vehicle (pH 2.6). Blood samples (~60 μL) were collected from the retro-orbital plexus at 0.08, 0.25, 0.5, 1, 4, and 8 h post i.v. dose and 0.25, 0.5, 1, 4, and 8 h post p.o. dose. The blood samples were collected from a set of three mice at each time point, and placed in microcentrifuge tubes containing a 20% K_2EDTA solution as an anticoagulant. The blood samples were then centrifuged at 4000 RPM for 10 min at 4 °C to separate the plasma. The plasma samples were stored at −80 °C prior to their bioanalysis. Plasma concentrations of TXY541 and PC190723 were quantified by LC–MS/MS, with the lower limit of quantitation (LLOQ) being 100.2 ng/mL for TXY541 and 10.1 ng/mL for PC190723. The time-dependent plasma concentration data were analyzed using the sparse sampling mode in the non-compartmental analysis (NCA) tool of the Phoenix WinNonlin® version 6.3 software package to yield relevant pharmacokinetic parameters.

2.10. In vivo *efficacy studies*

Antistaphylococcal efficacy *in vivo* was assessed in a mouse peritonitis model of systemic infection with *S. aureus* 8325-4 (MSSA), ATCC 19636 (MSSA), or ATCC 43300 (MRSA). These studies were conducted in full compliance with the standards established by the US National Research Council's Guide for the Care and Use of Laboratory Animals, and were approved by the Institutional Animal Care and Use Committee (IACUC) of Rutgers University. Groups of 6 female Swiss–Webster mice with an average weight of 25 g were infected intraperitoneally with a lethal inoculum of each bacterial strain in saline. The inocula of *S. aureus* 8325-4 and ATCC 43300 contained 5×10^7 CFUs of bacteria, while the inoculum of *S. aureus* ATCC 19636 contained 5×10^6 CFUs of bacteria. All the inocula also contained porcine mucin (Sigma–Aldrich, Co.) at a (w/v) percentage of 1.5% (in the 8325-4 and ATCC 19636 inocula) or 5% (in the ATCC 43300 inoculum). The differing compositions of the inocula of the three *S. aureus* strains were selected based on the virulence of each strain, with MSSA ATCC 19636 being the most virulent strain and MRSA ATCC 43300 being the least virulent strain. The reduced virulence of the MRSA strain relative to the MSSA strains is consistent with previously reported findings [35].

All compound and vehicle intravenous (i.v.) administrations were by tail vein injection, with TXY541 being formulated at 2.0 mg/mL in 10 mM citrate (pH 2.6). Four experimental groups of MSSA-infected mice were treated as follows: Group 1 – untreated; Group 2 – vehicle only; Group 3 – 96 mg/kg TXY541 (in four divided doses of 24 mg/kg); and Group 4 – 16 mg/kg vancomycin. The first dose of TXY541 was administered 1 min after infection, with subsequent doses being administered at 10-min intervals thereafter. The dosing volume for all the i.v. administrations was 8 mL/kg.

The mice were fasted overnight prior to their use in the oral (p.o.) studies. All compound and vehicle p.o. administrations were by gavage, with the vehicle also being 10 mM citrate (pH 2.6). Both TXY541 and PC190723 were formulated at 2.0 mg/mL, with the resulting TXY541 formulation being a solution and the resulting PC190723 formulation being a suspension. Four experimental groups of MSSA-infected mice were treated as follows: Group 1 – untreated; Group 2 – vehicle only; Group 3 – 128 mg/kg TXY541 (in four divided doses of 32 mg/kg); and Group 4 – 128 mg/kg PC190723 (in four divided doses of 32 mg/kg). The first dose of compound was administered 10 min after infection, with subsequent doses being administered at 12-min intervals thereafter. In the MRSA studies, three experimental groups of infected mice were treated as follows: Group 1 – untreated; Group 2 – vehicle only; and Group 3 – 192 mg/kg TXY541 (in six divided doses of 32 mg/kg). In these studies, the first dose of compound was administered one hour after infection, with subsequent doses being administered at 12-min intervals thereafter. The dosing volume for all the p.o. administrations was 16 mL/kg.

The body temperatures of all mice were monitored for a period of 5 days after infection. Body temperatures were recorded at the Xiphoid process using a noninvasive infrared thermometer (Braintree Scientific, Inc., Braintree, MA). Infected mice with body temperatures ≤28.9 °C were viewed as being unable to recover from the infection [36] and were euthanized.

2.11. Mammalian cytotoxicity studies

The cytotoxicity of TXY541 *versus* Vero cells (African green monkey kidney epithelial cells; ATCC) was assessed using a 72-h continuous 3-(4,5-dimethylthiazol-2-yl)-2,5-diphenyltetrazolium bromide (MTT) assay as described previously [37].

3. Results and discussion

3.1. TXY541 is associated with a 143-fold enhanced solubility relative to PC190723 in an acidic aqueous vehicle (10 mM citrate, pH 2.6) suitable for in vivo drug administration

We sought to determine whether the 1-methylpiperidine-4-carboxamide functionality on TXY541 afforded the compound enhanced aqueous solubility relative to PC190723. To this end, we used reverse-phase HPLC to determine the maximal solubility of TXY541 in two different aqueous vehicles suitable for *in vivo* drug administration [38,39], one at a physiological pH of 7.4 (PBS) and the other at an acidic pH of 2.6 (10 mM citrate). These studies yielded maximal TXY541 solubilities of 12.6 ± 1.4 μg/mL and 3220 ± 173 μg/mL in PBS and citrate, respectively (Table 1). Thus, TXY541 is 255-times more soluble in the acidic citrate vehicle than in the PBS vehicle at pH 7.4. We have previously shown that the maximal solubility of PC190723 is 23.9 ± 4.0 μg/mL in PBS and 22.5 ± 1.6 μg/mL in 10 mM citrate [40]. A comparison of these solubilities with the corresponding values for TXY541 reveals that TXY541 is approximately half as soluble as PC190723 in PBS. Thus, the 1-methylpiperidine-4-carboxamide functionality diminishes the aqueous solubility of TXY541 relative to PC190723 at physiological pH. In striking contrast, however, the 1-methylpiperidine-4-carboxamide functionality renders TXY541 143-times more soluble than PC190723 in the acidic citrate vehicle. Importantly, unlike PC190723, the solubility of TXY541 in this vehicle is sufficient in magnitude for *in vivo* efficacy studies of TXY541.

In addition to evaluating the solubility of TXY541 in the acidic citrate vehicle, we also assessed the chemical stability of the compound in the same vehicle using reverse-phase HPLC. Fig. 2 shows the HPLC chromatogram of 20 μM TXY541 after 24 h of incubation in the citrate vehicle at 37 °C. The corresponding chromatogram of 20 μM PC190723 is also shown for comparative purposes. Under the running conditions employed in our HPLC assays, TXY541 elutes at approximately 10.2 min after injection, while PC190723 elutes at approximately 11.7 min. The shorter retention time of TXY541 relative to PC190723 is consistent with its correspondingly decreased hydrophobicity (*C* log *P* = −0.38 for TXY541 *versus* +2.64 for PC190723; Fig. 1). Note that, even after 24 h of incubation, the chromatographic profile of TXY541 remains essentially unchanged, a result highlighting the chemical stability of TXY541 over this period of time in the acidic citrate vehicle.

3.2. TXY541 converts to PC190723 under physiological conditions, with the time dependence of this conversion being different in staphylococcal growth media versus mouse serum

We next sought to evaluate the time-dependent stability of TXY541 at 37 °C in two different physiological media at pH 7.4,

Table 1
Solubilities of TXY541 and PC190723 in 10 mM citrate and PBS at 25 °C[a].

Compound	Mean solubility (μg/mL) ± SD	
	Citrate (pH 2.6)	PBS (pH 7.4)
TXY541	3220 ± 173	12.6 ± 1.4
PC190723[b]	22.5 ± 1.6	23.9 ± 4.0

[a] Each solubility reflects the average of two independent determinations.
[b] Solubility values for PC190723 are taken from reference [40].

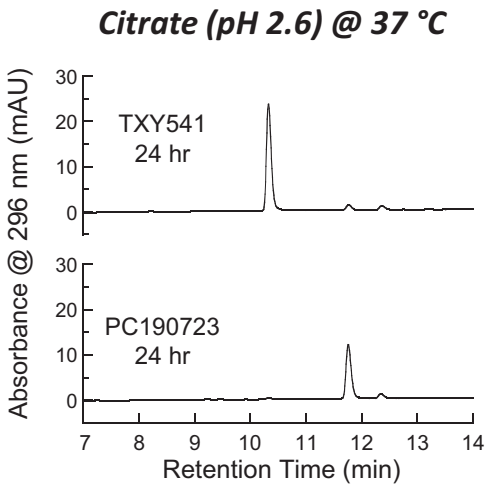

Fig. 2. Reverse-phase HPLC chromatogram of 20 μM TXY541 after 24 h of incubation at 37 °C in 10 mM citrate (pH 2.6). For comparative purposes, the corresponding chromatogram of 20 μM PC190723 is also presented.

CAMH broth (the media used for culturing *S. aureus*) and 100% filtered mouse serum. The left panel of Fig. 3 shows the HPLC chromatograms of 20 μM TXY541 after incubation in CAMH broth over a time period of 22 h. Note that over this time period, TXY541 fully converts to PC190723. Analysis of the TXY541 peak areas at the different time points yields a half-life for the conversion of 8.2 ± 0.4 h (Fig. 4A and B). Thus, TXY541 acts as an acid-soluble prodrug that converts to PC190723 under physiological pH conditions. We have previously shown that an *N*-Mannich base derivative of PC190723 (TXY436) also acts as a prodrug at physiological pH, converting to PC190723 with a half-life of approximately 18 min [40]. This conversion half-life is approximately 27-times faster than that of TXY541. Thus, the 1-methylpiperidine-4-carboxamide functionality affords TXY541 significantly greater stability at physiological pH than the *N*-Mannich base functionality affords TXY436.

We next investigated how the conversion of TXY541 to PC190723 in 100% mouse serum (also at pH 7.4) compared with that observed in CAMH broth. The right panel of Fig. 3 shows the HPLC chromatograms of 20 μM TXY541 after incubation in mouse serum for various times at 37 °C. Inspection of these chromatograms reveals that the conversion of TXY541 to PC190723 in mouse serum is complete within 30 min, a time period over which TXY541 remains essentially unconverted in CAMH broth (compare the 30-min chromatograms in the left and right panels of Fig. 3). The differing conversion kinetics of TXY541 in 100% mouse serum *versus* CAMH broth alone is highlighted by the analysis of the relevant TXY541 peak areas depicted in Fig. 4. This analysis yields a conversion half-life for TXY541 in mouse serum of 3.4 ± 0.2 min (Fig. 4D), a value approximately 145-times shorter than the observed conversion half-life in CAMH broth. In other words, the conversion of TXY541 to PC190723 is approximately 145-times faster in mouse serum than in CAMH broth. This striking differential implies that the conversion of TXY541 to PC190723 in mouse serum is induced by more than just the pH conditions, which occurs over a period of hours not minutes. It is therefore likely that the conversion in serum is predominantly catalyzed by one or more carboxyesterase and/or amidase enzymes that are present in serum. Future studies will be directed toward discerning the identities of the specific enzymes involved.

3.3. The TXY541 prodrug maintains the antistaphylococcal potency of PC190723 in the presence of mouse serum

We compared the antistaphylococcal activity of TXY541 and PC190723 in the absence and presence of 50% (v/v) mouse serum.

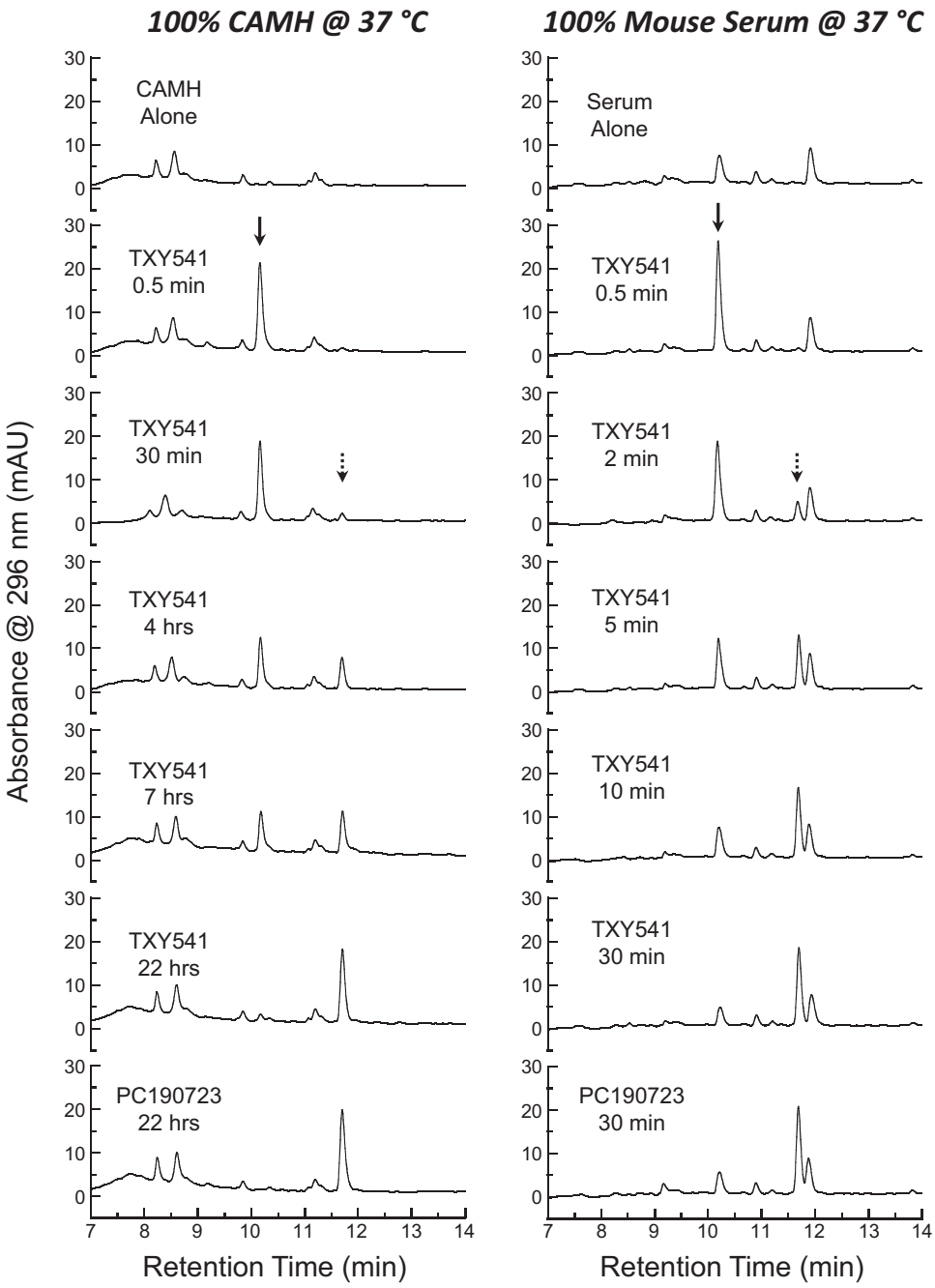

Fig. 3. Reverse-phase HPLC chromatograms of 20 μM TXY541 after the indicated times of incubation at 37 °C in either 100% cation-adjusted Mueller-Hinton (CAMH) broth, pH 7.4 (left panel) or 100% mouse serum, pH 7.4 (right panel). For comparative purposes, the corresponding chromatograms of 20 μM PC190723 after incubation for 22 h in CAMH broth (bottom of left panel) or 30 min in mouse serum (bottom of right panel) are also presented. The baseline chromatograms of CAMH broth and mouse serum alone are shown at the tops of the left and right panels, respectively. The solid arrows indicate the peak corresponding to TXY541, while the dashed arrows indicate the peak corresponding to PC190723.

Specifically, we used two different MSSA and two different MRSA strains in these evaluations, with the resulting MICs being summarized in Table 2. For all the MSSA and MRSA strains examined, the increased MIC of PC190723 in the presence (2.0 μg/mL) *versus* the absence (0.5 μg/mL) of serum suggests that PC190723 is approximately 75% bound to serum proteins in 50% mouse serum. Inspection of the data in Table 2 also reveals that the antistaphylococcal MICs of TXY541 in the absence and presence of serum are identical (2.0 μg/mL). Thus, compared to PC190723, the TXY541 prodrug exhibts reduced antistaphylococcal potency in the absence of serum, but identical potency in the presence of serum. Recall that the conversion of TXY541 to PC190723 occurs approximately 145-times more rapidly in mouse serum than in CAMH broth with no serum. The slow rate of conversion in CAMH broth alone likely accounts for the reduced antistaphylococcal potency of TXY541 relative to PC190723 in the absence of serum, since the MICs for TXY541 determined under these conditions reflect the mixed presence of both the TXY541 prodrug itself as well as the PC190723 product. By extension, these MIC results also imply that any intrinsic antistaphylococcal activity associated with the TXY541 prodrug must be lower than that of the PC109723 product.

With regard to the two MRSA strains used in the studies, the activity of TXY541 was comparable to the activity of the

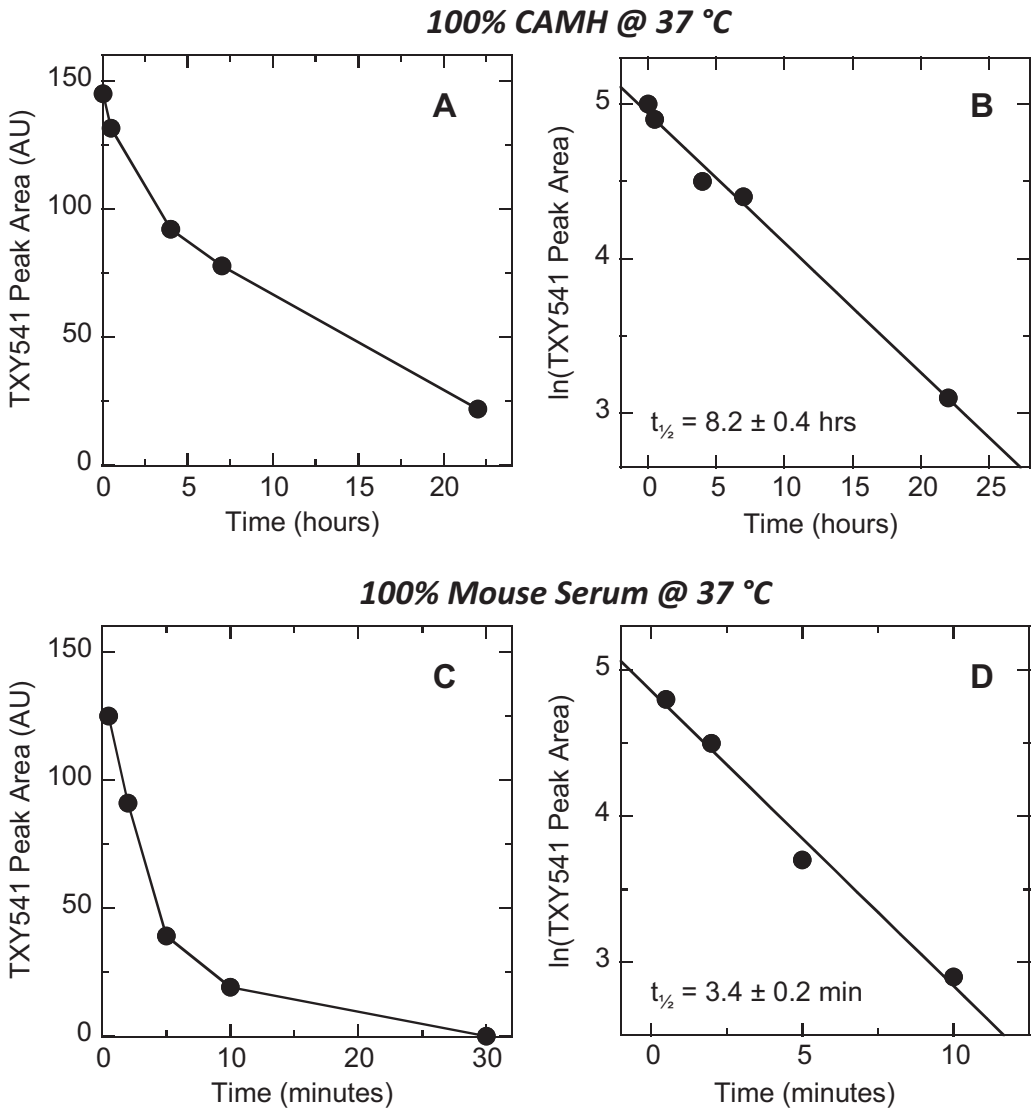

Fig. 4. (A and C) Time-dependence of integrated HPLC peak areas for TXY541 after incubation at 37 °C in 100% CAMH broth (A) or 100% mouse serum (C). AU denotes arbitrary units. (B and D) Plot of ln(TXY541 peak area) *versus* time at 37 °C in 100% CAMH broth (B) or 100% mouse serum (D). The indicated half-lives ($t_{½}$) for the conversion of TXY541 to PC190723 were determined using the relationship, $t_{½} = -0.693/m$, where m is the slope derived from the linear least squares fit of the experimental data points (as indicated by the solid lines). The uncertainty in $t_{½}$ reflects the maximal error in m propagated through the above relationship.

prototypical anti-MRSA drug vancomycin (MIC = 2.0 μg/mL), which was included as a comparator antibiotic. Oxacillin (also included as a control antibioitc) was predictably inactive *versus* the MRSA strains (MIC > 64 μg/mL).

3.4. The antistaphylococcal activity of TXY541 is bactericidal in nature

We next sought to determine whether the antistaphylococcal activity of TXY541 is bactericidal or bacteriostatic in nature. To this end, we determined the MBC values of TXY541 against the two MSSA strains (8325-4 and ATCC 19636) and the two MRSA strains (ATCC 33591 and 43300). The bactericidal antistaphylococcal drug vancomycin and the bacteriostatic drug erythromycin were used as comparator controls in these determinations. As per CLSI standards, an MBC/MIC ratio of 1 to 2 is considered indicative of bactericidal behavior [33]. By contrast, an MBC/MIC ratio >8 is viewed as being indicative of bacteriostatic behavior. As expected, the control bactericidal agent vancomycin yielded MBC/MIC ratios

Table 2
Antistaphylococcal activities of TXY541 and PC190723 in the absence and presence of mouse serum.[a]

Compound	MIC *vs. S. aureus* (μg/mL)							
	8325-4 (MSSA)		ATCC 19636 (MSSA)		ATCC 43300 (MRSA)		ATCC 33591 (MRSA)	
	No serum	50% mouse serum	No serum	50% mouse serum	No serum	50% mouse serum	No serum	50% mouse serum
TXY541	2.0	2.0	2.0	2.0	2.0	2.0	2.0	2.0
PC190723	0.5	2.0	0.5	2.0	0.5	2.0	0.5	2.0
Vancomycin	1.0	2.0	1.0	2.0	2.0	2.0	2.0	2.0
Oxacillin	0.13	0.5	0.13	0.5	>64	>64	>64	>64

[a] Vancomycin and oxacillin are included as control antistaphylococcal agents.

Table 3
Comparison of MIC and MBC values for TXY541 against methicillin-sensitive and methicillin-resistant strains of *S. aureus*.[a]

Compound	MIC (μg/mL)	MBC (μg/mL)	MBC/MIC
8325-4 (MSSA)			
TXY541	2.0	4.0	2
Vancomycin	1.0	2.0	2
Erythromycin	0.125	32	256
19636 (MSSA)			
TXY541	2.0	4.0	2
Vancomycin	1.0	1.0	1
Erythromycin	0.5	>64	>128
33591 (MRSA)			
TXY541	2.0	4.0	2
Vancomycin	2.0	4.0	2
Erythromycin	>64	na	na
43300 (MRSA)			
TXY541	2.0	4.0	2
Vancomycin	2.0	4.0	2
Erythromycin	>64	na	na

na, not applicable.
[a] Vancomycin and erythromycin are included as control bactericidal and bacteriostatic agents, respectively.

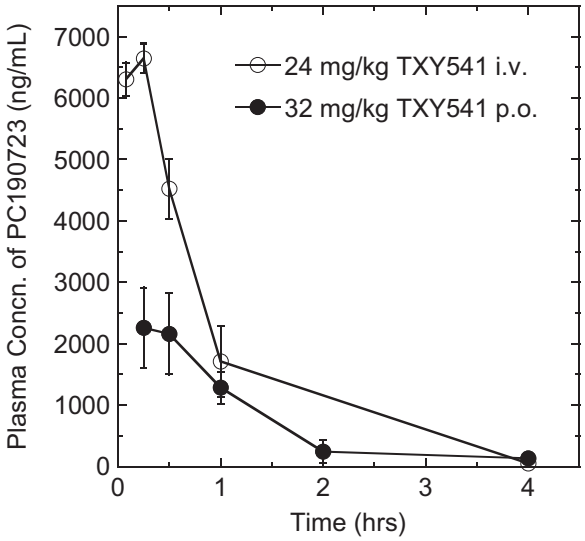

Fig. 5. Time-dependent plasma concentrations of PC190723 following either a single i.v. administration of 24 mg/kg TXY541 (open circles) or a single p.o. administration of 32 mg/kg TXY541 (filled circles) to male BALB/c mice.

of 1 to 2 against all the MSSA and MRSA strains examined (Table 3). Also as expected, the control bacteriostatic drug erythromycin yielded MBC/MIC ratios >128 against the two MSSA strains. Both MRSA strains were resistant to erythromycin, precluding MBC determinations against these strains. Significantly, TXY541 exhibited MBC/MIC ratios of 1 to 2 against all the MSSA and MRSA strains, indicative of bactericidal antistaphylococcal behavior.

3.5. The staphylococcal frequency of resistance (FOR) to TXY541 is similar to that observed with PC190723

PC190723 has been reported to be associated with a frequency of resistance (FOR) in *S. aureus* of approximately 3×10^{-8} [17,41]. We sought to determine the corresponding FOR to TXY541 in *S. aureus* using a large inoculum approach. These studies yielded an FOR to TXY541 of $(1.0 \pm 0.4) \times 10^{-8}$, a value similar in magnitude to that reported for PC190723. This similarity is not surprising, as the majority of the TXY541 prodrug is converted to the PC190723 product under the conditions employed in the FOR determinations.

3.6. Pharmacokinetic analysis of the TXY541 prodrug and its PC190723 product following intravenous or oral administration of TXY541 to mice

As a prelude to conducting *in vivo* efficacy experiments, we sought to evaluate the plasma pharmacokinetics of the TXY541 prodrug and its PC190723 product following intravenous (i.v.) or oral (p.o.) administration of TXY541 to mice. In these studies, a single i.v. dose of 24 mg/kg or p.o. dose of 32 mg/kg was administered to mice and plasma concentrations of TXY541 and PC190723 were measured at time points ranging from 0.08 to 8 h using LC–MS/MS. No TXY541 was detectable in the plasma at any time point by either route of administration. By contrast, the plasma concentration of PC190723 was detectable and quantifiable up to 4 h following both i.v. and p.o. administration. This observation is consistent with the rapid conversion of TXY541 to PC190723 that we observed in the presence of 100% mouse serum at 37 °C (Figs. 3 and 4).

The time-dependent plasma concentrations of PC190723 after both p.o. and i.v. administration of TXY541 are graphically depicted in Fig. 5. Pharmacokinetic analysis of these time-dependent plasma concentration data yielded the pharmacokinetic parameters listed in Table 4. Analysis of the PC190723 plasma concentrations after i.v. administration of TXY541 yielded an elimination half-life ($t_{½}$) of approximately 0.6 h and a moderate total body clearance (CL) of 55.1 mL/min-kg, approximately 61% that of normal liver blood flow in mice (90 mL/min-kg). The volume of distribution at steady state (V_{ss}) was found to be 2.18 L/kg. Significantly, this value of V_{ss} is approximately 3-times greater than that of normal body water (0.7 L/kg), indicating the extravascular distribution of PC190723. This degree of extravascular distribution on the part of PC190723 is not surprising given the lipophilic nature of the compound ($C \log P = 2.64$).

Upon oral administration of TXY541, the peak plasma concentration of PC190723 was achieved within 15 min ($t_{max} = 0.25$ h). A comparison of the areas under the curves up to the last detectable concentrations of PC190723 (AUC_{last}) following both p.o. and i.v. administration of TXY541 yields an oral bioavailability (%*F*) for PC190723 of 29.6% after normalization for dose. Thus, unlike many clinical MRSA drugs, including vancomycin, daptomycin, and the streptogramins, TXY541 is orally bioavailable.

Table 4
Pharmacokinetic parameters of the PC190723 product following a single intravenous (i.v.) or oral (p.o.) administration of the TXY541 prodrug to male BALB/c mice.[a]

Route of administration	Dose of TXY541 (mg/kg)	t_{max} (h)	C_0[b] (ng/L)	AUC_{last} (ng/L-h)	AUC_{inf} (ng/L-h)	$t_{½}$ (h)	CL (mL/min-kg)	V_{ss} (L/kg)	%*F*[c]
i.v.	24	na	6308	7216	7258	0.56	55.1	2.18	na
p.o.	32	0.25	2263	2848	3016	na	na	na	29.6

[a] Parameters were calculated by analysis of the plasma concentration *versus* time plots shown in Fig. 5 using the sparse sampling mode in the NCA module of the Phoenix WinNonlin v6.3 software package na, not applicable.
[b] Extrapolated concentration for i.v. group.
[c] AUC_{last} was used for calculation of %*F*.

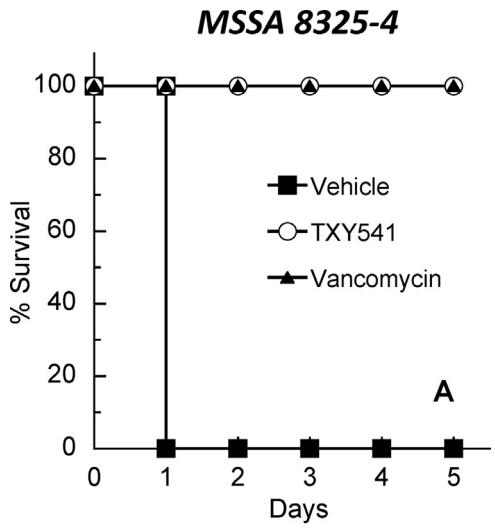

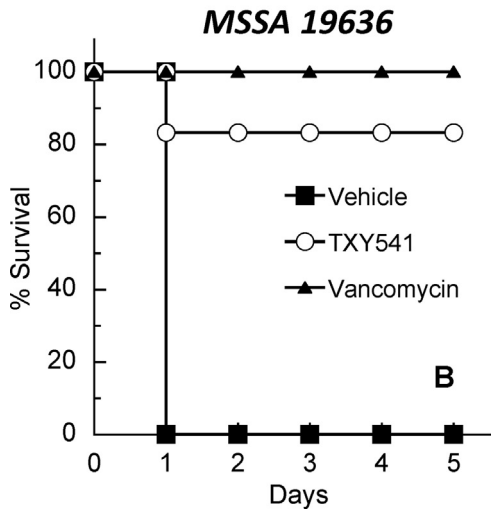

Fig. 6. Intravenous (i.v.) *in vivo* efficacy of TXY541 against systemic MSSA infection with *S. aureus* 8325-4 (A) or ATCC 19636 (B). TXY541 was administered at a dose of 96 mg/kg (in four divided doses). As a positive control, vancomycin was administered i.v. at a dose of 16 mg/kg. The vehicle was 10 mM citrate (pH 2.6) in all experiments.

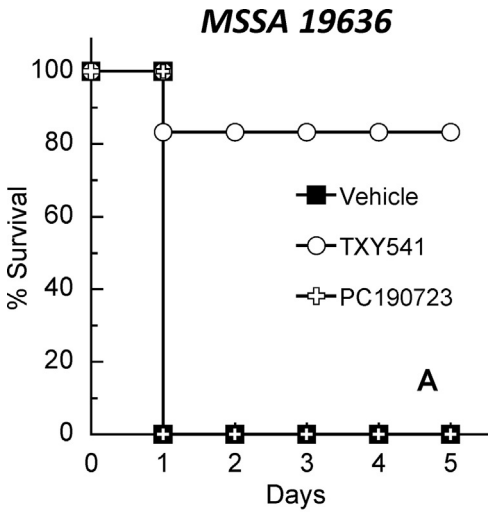

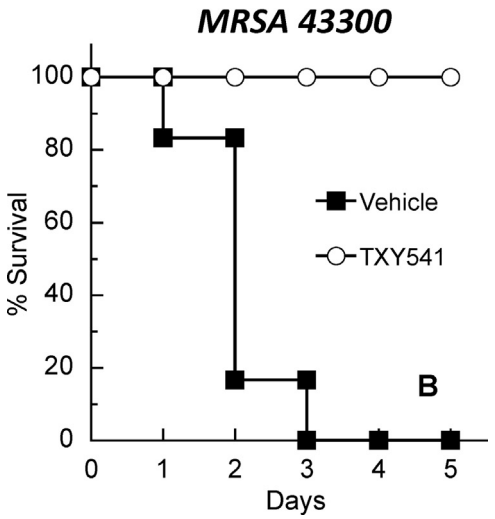

Fig. 7. Oral (p.o.) *in vivo* efficacy of TXY541 against systemic infection with either MSSA ATCC19636 or MRSA ATCC 43300. In the MSSA experiments, TXY541 and PC190723 were administered at 128 mg/kg in four divided doses. In the MRSA experiments, TXY541 was administered at 192 mg/kg in six divided doses. The vehicle was 10 mM citrate (pH 2.6) in all experiments.

3.7. When administered either intravenously or orally, TXY541 is efficacious in vivo against systemic MSSA and MRSA infections

Armed with the pharmacokinetic results described above, we next evaluated the *in vivo* antistaphylococcal efficacy of TXY541 using a mouse peritonitis model of systemic infection with *S. aureus*. In our initial studies, mice were inoculated intraperitoneally with a lethal inoculum of MSSA (either strain 8325-4 or ATCC 19636) in 1.5% mucin. The mice were either left untreated, treated i.v. with vehicle (10 mM citrate, pH 2.6) alone, or treated i.v. with 96 mg/kg TXY541 (in four divided doses of 24 mg/kg).

None of the mice treated with citrate vehicle alone survived beyond a day post infection (Fig. 6). By contrast, ≥83% of the mice treated with TXY541 survived the MSSA infections. Vancomycin was used as a positive control in these i.v. studies and yielded its expected salutary impact on survival.

We next sought to determine whether the *in vivo* efficacy of TXY541 against systemic MSSA infection would also be observed when the compound is administered orally. To this end, TXY541 or PC190723 were administered p.o. to mice infected with MSSA strain ATCC 19636. In these studies, the compounds were administered at a dose of 128 mg/kg (in four divided doses of 32 mg/kg). Note that the poor solubility of PC190723 in the citrate vehicle mandated that this compound be administered as a suspension rather than as a solution like TXY541. The results from these studies are shown in Fig. 7A. Once again, none of the mice treated with citrate vehicle alone survived beyond one day post infection. As observed in the i.v. studies, 83% of the mice treated p.o. with TXY541 survived the infection. Thus, the TXY541 prodrug is not only efficacious against systemic MSSA infection when administered intravenously, but also when administered orally. In marked contrast to TXY541, p.o. treatment with PC190723 was not efficacious, failing to yield any survivors beyond one day post infection. This lack of efficacy on the part of PC190723 may be due to the poor solubility of the compound in the citrate vehicle, which mandated that the compound be administered as a suspension rather than a solution.

In our next series of studies, we sought to determine whether the oral antistaphylococcal efficacy of TXY541 would extend beyond MSSA infections to include MRSA infections as well. In these studies, mice were inoculated intraperitoneally with a lethal inoculum of MRSA ATCC 43300 in 5% mucin. The mice were either left untreated, treated p.o. with citrate vehicle alone, or treated p.o. with 192 mg/kg TXY541 (in six divided doses of 32 mg/kg). None of

the vehicle-treated mice survived beyond three days post infection (Fig. 7B). By contrast, 100% of the mice treated with TXY541 survived the infection. Thus, the TXY541 prodrug is not only orally efficacious against systemic MSSA infections, but also against systemic MRSA infections.

3.8. TXY541 is minimally toxic to mammalian cells

To probe for any potential mammalian cytotoxicity, we used a 3-day tetrazole (MTT)-based assay to assess the cytotoxicity of TXY541 against Vero, African green monkey kidney epithelial cells. TXY541 was found to be minimally toxic to Vero cells, with an IC_{50} of >128 μg/mL. Significantly, this IC_{50} value is >64-times the antistaphylococcal MIC values of TXY541 (2.0 μg/mL). This promising initial result suggests that TXY541 may be associated with a significant therapeutic window. Future studies with additional mammalian and human cell lines will be directed toward assessing the general nature of this result.

4. Conclusions

In conclusion, our results indicate that the 1-methylpiperidine-4-carboxamide derivative TXY541 acts as a prodrug of the FtsZ-targeting benzamide PC190273. It is associated with enhanced formulation properties compared to PC190723 itself, which, in turn, confer the prodrug with efficacy *in vivo* against both MSSA and MRSA systemic infections. The *in vivo* antistaphylococcal efficacy of TXY541 is not only observed when the compound is administered intravenously, but also when it is administered orally. This result is significant, as few anti-MRSA agents in current clinical use are orally bioavailable. The *in vitro* and *in vivo* antistaphylococcal properties of TXY541, coupled with its minimal cytotoxicity *versus* mammalian cells, warrant further investigation of the compound as a potentially useful agent for the treatment of MSSA and MRSA infections.

Acknowledgements

This study was supported by research agreements between TAXIS Pharmaceuticals, Inc. and both Rutgers Robert Wood Johnson Medical School (D.S.P.) and Rutgers Ernest Mario School of Pharmacy (E.J.L.). We are indebted to Dr. Nancy Connell (Rutgers New Jersey Medical School, Newark, NJ) for her assistance with the mammalian cytotoxicity studies. We are also indebted to Dr. Glenn W. Kaatz (John D. Dingell VA Medical Center, Detroit, MI) for providing us with the *S. aureus* 8325-4 strain.

References

[1] Arias CA, Murray BE. Antibiotic-resistant bugs in the 21st century – a clinical super-challenge. New Engl J Med 2009;360:439–43.
[2] Livermore DM. Fourteen years in resistance. Int J Antimicrob Agents 2012;39:283–94.
[3] Moellering Jr RC. MRSA. The first half century. J Antimicrob Chemother 2012;67:4–11.
[4] Otto M. MRSA virulence and spread. Cell Microbiol 2012;14:1513–21.
[5] Bi EF, Lutkenhaus J. FtsZ ring structure associated with division in *Escherichia coli*. Nature 1991;354:161–4.
[6] Adams DW, Errington J. Bacterial cell division: assembly, maintenance and disassembly of the Z ring. Nat Rev Microbiol 2009;7:642–53.
[7] Erickson HP, Anderson DE, Osawa M. FtsZ in bacterial cytokinesis: cytoskeleton and force generator all in one. Microbiol Mol Biol Rev 2010;74:504–28.
[8] Lutkenhaus J, Addinall SG. Bacterial cell division and the Z ring. Annu Rev Biochem 1997;66:93–116.
[9] Egan AJ, Vollmer W. The physiology of bacterial cell division. Ann NY Acad Sci 2013;1277:8–28.
[10] Kirkpatrick CL, Viollier PH. New(s) to the (Z-)ring. Curr Opin Microbiol 2011;14:691–7.
[11] Lutkenhaus J, Pichoff S, Du S. Bacterial cytokinesis: from Z ring to divisome. Cytoskeleton 2012;69:778–90.
[12] Addinall SG, Bi E, Lutkenhaus J. FtsZ ring formation in *fts* mutants. J Bacteriol 1996;178:3877–84.
[13] Dai K, Lutkenhaus J. FtsZ is an essential cell division gene in *Escherichia coli*. J Bacteriol 1991;173:3500–6.
[14] Adams DW, Wu LJ, Czaplewski LG, Errington J. Multiple effects of benzamide antibiotics on FtsZ function. Mol Microbiol 2011;80:68–84.
[15] Awasthi D, Kumar K, Ojima I. Therapeutic potential of FtsZ inhibition: a patent perspective. Expert Opin Ther Pat 2011;21:657–79.
[16] Haydon DJ, Bennett JM, Brown D, Collins I, Galbraith G, Lancett P, et al. Creating an antibacterial with *in vivo* efficacy: synthesis and characterization of potent inhibitors of the bacterial cell division protein FtsZ with improved pharmaceutical properties. J Med Chem 2010;53:3927–36.
[17] Haydon DJ, Stokes NR, Ure R, Galbraith G, Bennett JM, Brown DR, et al. An inhibitor of FtsZ with potent and selective anti-staphylococcal activity. Science 2008;321:1673–5.
[18] Huang Q, Kirikae F, Kirikae T, Pepe A, Amin A, Respicio L, et al. Targeting FtsZ for antituberculosis drug discovery: noncytotoxic taxanes as novel antituberculosis agents. J Med Chem 2006;49:463–6.
[19] Huang Q, Tonge PJ, Slayden RA, Kirikae T, Ojima I. FtsZ: a novel target for tuberculosis drug discovery. Curr Top Med Chem 2007;7:527–43.
[20] Kapoor S, Panda D. Targeting FtsZ for antibacterial therapy: a promising avenue. Expert Opin Ther Targets 2009;13:1037–51.
[21] Kaul M, Parhi AK, Zhang Y, LaVoie EJ, Tuske S, Arnold E, et al. A bactericidal guanidinomethyl biaryl that alters the dynamics of bacterial FtsZ polymerization. J Med Chem 2012;55:10160–76.
[22] Kumar K, Awasthi D, Berger WT, Tonge PJ, Slayden RA, Ojima I. Discovery of anti-TB agents that target the cell-division protein FtsZ. Future Med Chem 2010;2:1305–23.
[23] Kumar K, Awasthi D, Lee SY, Zanardi I, Ruzsicska B, Knudson S, et al. Novel trisubstituted benzimidazoles, targeting *Mtb* FtsZ, as a new class of antitubercular agents. J Med Chem 2011;54:374–81.
[24] Lock RL, Harry EJ. Cell-division inhibitors: new insights for future antibiotics. Nat Rev Drug Discov 2008;7:324–38.
[25] Ma S. The development of FtsZ inhibitors as potential antibacterial agents. ChemMedChem 2012;7:1161–72.
[26] Schaffner-Barbero C, Martin-Fontecha M, Chacón P, Andreu JM. Targeting the assembly of bacterial cell division protein FtsZ with small molecules. ACS Chem Biol 2012;7:269–77.
[27] Stokes NR, Baker N, Bennett JM, Berry J, Collins I, Czaplewski LG, et al. An improved small-molecule inhibitor of FtsZ with superior in vitro potency, drug-like properties, and in vivo efficacy. Antimicrob Agents Chemother 2013;57:317–25.
[28] Anderson DE, Kim MB, Moore JT, O'Brien TE, Sorto NA, Grove CI, et al. Comparison of small molecule inhibitors of the bacterial cell division protein FtsZ and identification of a reliable cross-species inhibitor. ACS Chem Biol 2012;7:1918–28.
[29] Kaul M, Zhang Y, Parhi AK, Lavoie EJ, Tuske S, Arnold E, et al. Enterococcal and streptococcal resistance to PC190723 and related compounds: molecular insights from a FtsZ mutational analysis. Biochimie 2013;95:1880–7.
[30] Andreu JM, Schaffner-Barbero C, Huecas S, Alonso D, Lopez-Rodriguez ML, Ruiz-Avila LB, et al. The antibacterial cell division inhibitor PC190723 is an FtsZ polymer-stabilizing agent that induces filament assembly and condensation. J Biol Chem 2010;285:14239–46.
[31] Kaatz GW, Seo SM, O'Brien L, Wahiduzzaman M, Foster TJ. Evidence for the existence of a multidrug efflux transporter distinct from NorA in *Staphylococcus aureus*. Antimicrob Agents Chemother 2000;44:1404–6.
[32] Sorto NA, Olmstead MM, Shaw JT. Practical synthesis of PC190723, an inhibitor of the bacterial cell division protein FtsZ. J Org Chem 2010;75:7946–9.
[33] CLSI. Methods for dilution antimicrobial susceptibility tests for bacteria that grow aerobically. Approved Standard-eighth ed. Wayne, PA: Clinical and Laboratory Standards Institute; 2009.
[34] O'Neill AJ, Cove JH, Chopra I. Mutation frequencies for resistance to fusidic acid and rifampicin in *Staphylococcus aureus*. J Antimicrob Chemother 2001;47:647–50.
[35] Mizobuchi S, Minami J, Jin F, Matsushita O, Okabe A. Comparison of the virulence of methicillin-resistant and methicillin-sensitive *Staphylococcus aureus*. Microbiol Immunol 1994;38:599–605.
[36] Stiles BG, Campbell YG, Castle RM, Grove SA. Correlation of temperature and toxicity in murine studies of staphylococcal enterotoxins and toxic shock syndrome toxin 1. Infect Immun 1999;67:1521–5.
[37] Ekins S, Reynolds RC, Kim H, Koo M-S, Ekonomidis M, Talaue M, et al. Bayesian models leveraging bioactivity and cytotoxicity information for drug discovery. Chem Biol 2013;20:370–8.
[38] Li P, Zhao L. Developing early formulations: practice and perspective. Int J Pharm 2007;341:1–19.
[39] Turner PV, Pekow C, Vasbinder MA, Brabb T. Administration of substances to laboratory animals: equipment considerations, vehicle selection, and solute preparation. J Am Assoc Lab Anim Sci 2011;50:614–27.
[40] Kaul M, Mark L, Zhang Y, Parhi AK, LaVoie EJ, Pilch DS. A FtsZ-targeting prodrug with oral antistaphylococcal efficacy *in vivo*. Antimicrob Agents Chemother 2013;57. http://dx.doi.org/10.1128/AAC.01016-13.
[41] Tan CM, Therien AG, Lu J, Lee SH, Caron A, Gill CJ, et al. Restoring methicillin-resistant *Staphylococcus aureus* susceptibility to β-lactam antibiotics. Sci Transl Med 2012;4:126ra135.